Pattern Anal Applic (2015) 18:31–44
DOI 10.1007/s10044-013-0345-7

ORIGINAL ARTICLE

A novel hybrid intelligent system for multi-objective machine parameter optimization

Raquel Redondo · Javier Sedano · Vicente Vera · Beatriz Hernando · Emilio Corchado

Received: 6 June 2012 / Accepted: 17 June 2013 / Published online: 6 July 2013

Abstract This multidisciplinary research presents a novel hybrid intelligent system to perform a multi-objective industrial parameter optimization process. The intelligent system is based on the application of evolutionary and neural computation in conjunction with identification systems, which makes it possible to optimize the implementation conditions in the manufacturing process of high precision parts, including finishing precision, while saving time, financial costs and/or energy. Empirical verification of the proposed hybrid intelligent system is performed in a real industrial domain, where a case study is defined and analyzed. The experiments are carried out based on real dental milling processes using a high precision machining centre with five axes, requiring high finishing precision of measures in micrometers with a large number of process factors to analyze. The results of the experiments which validate the performance of the proposed approach are presented in this study.

Keywords Hybrid intelligent system · Dental milling process · Optimization · Unsupervised learning · Identification systems · Multi-objective optimization

R. Redondo (✉)
Department of Civil Engineering, University of Burgos, Burgos, Spain
e-mail: rredondo@ubu.es

J. Sedano
Department of AI and Applied Electronics, Castilla y León Technological Institute, Burgos, Spain
e-mail: javier.sedano@itcl.es

V. Vera · B. Hernando
Facultad de Odontología, UCM, Madrid, Spain
e-mail: viventevera@odon.ucm.es

E. Corchado
Department de Informática y Automática, Universidad de Salamanca, Salamanca, Spain
e-mail: escorchado@usal.es

E. Corchado
IT4Innovations, Ostrava, Czech Republic

1 Introduction

Intelligent systems have been widely used for industrial process modelling. Recently, different paradigms of artificial intelligence have been applied to different industrial problems [1–3].

System identification [4–6] has made it possible to model, simulate and predict the behavior of many industrial applications successfully and in different areas, such as control, robotics [7], energy processes [8], milling machine [9], high precision [1], power system security [10], etc. A novel and economically advantageous application is the optimization process in the field of Medical Therapeutics (Odonto-Stomatology), a booming industry [9, 11–13].

Prosthetic restorations must have a high marginal fit [14]. A bad marginal fit [15] affects fracture resistance and reduces the longevity of the restoration, resulting in higher risk of recurrent carious lesions and periodontal disease, as well as the dissolution of the cement [16] which allows entry of fluid and microorganisms between the tooth and the restoration, causing discoloration, pulpal irritation, secondary carious lesions and treatment failure [17].

Disturbances or marginal discrepancies between 50 and 120 micrometers are considered clinically acceptable in relation to the longevity of the restorations [18, 19].

Improved processing and optimization of parameters, such as processing time, temperature, accuracy, etc., for the development of pieces (such as dental-oral prostheses for partial crowns, inlays, onlays, etc., with application for rehabilitation and oral-dental restoration) are the focus of rigorous studies today [9]. The optimization process of machine parameters, such as the time parameter [20], permits significant economic savings due to the high number of dental pieces produced daily by the same high precision dental milling machine centre. Another important factor in the milling process is the temperature of the tools, which can be expanded or fractured by an inappropriate feed rate or by the heating of the coolant. Maintaining a constant temperature during the manufacturing process will make it possible to produce dental pieces with suitable quality. This could significantly help to increase a company's efficiency, and substantially contribute to cost reductions in the preparation and setting of the machines processes.

One way to achieve this optimization is based on the hybridization [9, 21–25] of emerging and active techniques, such as neural [5, 25] and evolutionary computation [26, 27], nature-inspired smart systems [28], data mining and decision support systems [29], information fusion [30], ensemble models, visualization techniques [31], cognitive and reactive distributed AI systems [32], case-based reasoning [33], among others.

This study is organized as follows. Section 2 describes hybrid intelligent systems. Section 3 introduces the unsupervised neural models applied for analyzing the data sets. Section 4 presents the system identification techniques used in the system modelling. Section 5 introduces the applied multi-objective genetic algorithm. Section 6 presents the hybrid intelligent system for the optimization of the process. Section 7 describes the industrial case study, a real dental milling process. The final section presents the different models that are used to solve the high precision dental milling optimization case study. At the end, the conclusions are set out and some comments on future research lines are presented.

2 Hybrid intelligent systems

The hybridization of intelligent techniques [9, 21–25] from different computational intelligence fields is becoming more and more popular due the growing awareness that such combinations frequently perform better than the individual techniques from computational intelligence (evolutionary [26, 27] and neurocomputing [5, 25], fuzzy systems [4], and so on).

Practical experience has indicated that hybrid intelligence techniques might be helpful to solve some of the challenging real-world problems. In a hybrid intelligence system, a synergistic combination of multiple techniques is used to build an efficient solution of a specific problem.

3 Exploratory projection pursuit

In this study, an extension of a neural principal component analysis (PCA) version [34–36] and other exploratory projection pursuit (EPP) [37–39] versions are used initially to select the most relevant input features in the data set, and secondly to study its internal structure.

Feature selection [40, 41] describes the tools and techniques available for reducing inputs to a manageable size for processing and analysis.

The feature selection approach in this study is based on the issue of dimension reduction. Initially, some projection methods, such as PCA [34–36], maximum likelihood Hebbian learning (MLHL) [38] and cooperative maximum likelihood Hebbian learning (CMLHL) [31, 42] are applied. Their first step is to analyze the internal structure of a representative data set from a case study. If after applying these models, a clear internal structure can be identified, this means that the data recorded is informative enough. Otherwise, further data must be properly collected [20].

Principal component analysis is a statistical model [34, 35] which describes the variation in a set of multivariate data in terms of a set of uncorrelated variables, each of which is a linear combination of the original variables.

Its goal is to derive new variables, in decreasing order of importance, that are linear combinations of the original variables and are uncorrelated with each other.

Using PCA, it is possible to find a smaller group of underlying variables that describe the data. PCA has been the most frequently reported linear operation involving unsupervised learning for data compression and feature selection [36].

3.1 A connectionist implementation of exploratory projection pursuit

Exploratory projection pursuit [37–39] is a more recent statistical method aimed at solving the difficult problem of identifying structure in high-dimensional data. It does this by projecting the data onto a low-dimensional subspace in which the data structure is searched by eye. However, not all projections will reveal this structure equally well. It therefore defines an index that measures how "interesting" a given projection is, and then represents the data in terms of projections that maximize the index.

The first step for EPP is to define which indexes represent interesting directions. "Interestingness" is usually

defined with respect to the fact that most projections of high-dimensional data give almost Gaussian distributions [37]. Thus, to identify "interesting" features in data, it is appropriate to look for those directions in which the data projections are as far from the Gaussian as possible.

Kurtosis is based on the normalized fourth moment and measures the heaviness of the tails of a distribution. A bimodal distribution will often have a negative kurtosis, which will therefore signal that a particular distribution shows evidence of clustering.

If a Gaussian distribution with mean a and variance x is as interesting as a Gaussian distribution with mean b and variance y, then such information may be removed from the data (sphering). In effect, the second-order structure can obscure structures of a higher order that are more interesting.

Cooperative maximum likelihood Hebbian learning [42] is based on MLHL [43], an EPP connectionist model. CMLHL includes lateral connections [42, 44] derived from the rectified Gaussian distribution (RGD) [45]. The RGD is a modification of the standard Gaussian distribution in which the variables are constrained to be non-negative, enabling the use of non-convex energy functions. The CMLHL architecture is depicted in Fig. 1, where lateral connections are highlighted.

The lateral connections used by CMLHL are based on the cooperative distribution mode that is closely spaced along a non-linear continuous manifold. Consequently, the resultant net can find the independent factors of a data set in a way that captures some type of global ordering.

Considering an N-dimensional input vector (x), an M-dimensional output vector (y) and with W_{ij} being the weight (linking input j to output i), CMLHL can be expressed as:

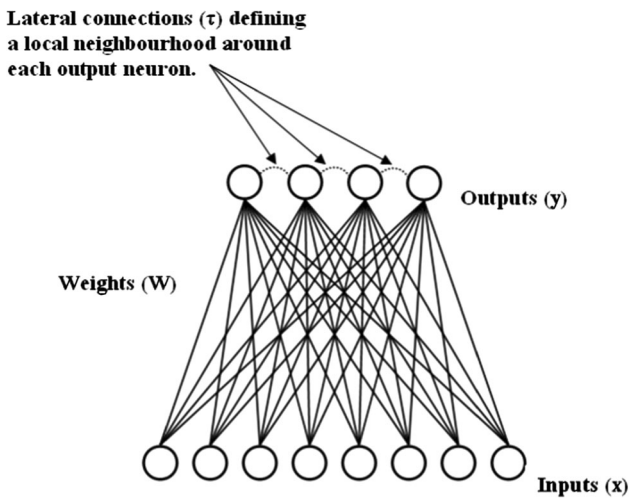

Fig. 1 CMLHL: lateral connections between neighboring output neurons

Feedforward step:

$$y_i = \sum_{j=1}^{N} W_{ij} x_j, \quad \forall i \tag{1}$$

Lateral activation passing:

$$y_i(t+1) = [y_i(t) + \tau(b - Ay)]^+ \tag{2}$$

Feedback step:

$$e_j = x_j - \sum_{i=1}^{M} W_{ij} y_i, \quad \forall j \tag{3}$$

Weight change:

$$\Delta W_{ij} = \eta . y_i . \text{sign}\ (e_j) |e_j|^p \tag{4}$$

where η is the learning rate, τ is the "strength" of the lateral connections, b the bias parameter, and p is a parameter related to the energy function [42, 43].

A is a symmetric matrix used to modify the response to the data, the effect of which is based on the relation between the distances between the output neurons. It is based on Cooperative Distribution, but to speed up the learning process, it can be simplified to:

$$A(i,j) = \delta_{ij} - \cos(2\pi(i-j)/M) \tag{5}$$

where, $\delta_{ij}$is the Kronecker delta.

4 System modelling using identification algorithms

System identification (SI) [4–6] aims to obtain mathematical models to estimate the behavior of a physical process whose dynamic equations are unknown. The identification criterion consists of evaluating the group of candidate models that best describes the data set gathered for the experiment. The goal is to obtain a model that meets the following premise [6]: a good model is one that makes good predictions and produces small errors when the observed data is applied.

Classic SI refers to the parametrical literature, which has its origin in linear system analysis [7]. Nevertheless, increased computational capability and the availability of soft computing techniques have widened research into SI. Artificial neural networks (ANN) are one of the paradigms used in SI [46]. When using ANN, the purpose of an identification process is to determine the weight matrix based on the observations Z^t, so as to obtain the relationships between the network nodes. The SI procedure comprises several steps: the selection of the models and their structure, the learning methods, the identification and optimization criteria and the validation method [6, 7, 46, 47]. Validation ensures that the selected model meets the necessary conditions for estimation and prediction. Typically, validation is carried out using three different

methods: the residual analysis $\varepsilon(t, \hat{\theta}(t))$ (by means of a correlation test between inputs, their residuals and their combinations), the mean squared error (MSE) and the generalization error value [normalized sum of squared errors (NSSE)], and finally a graphical comparison between the desired outputs and the model outcomes through simulation [7, 20].

5 Multi-objective optimization

Multi-objective optimization [48, 49] deals with solving optimization problems which involve multiple objectives, there is usually no single solution which is optimum with respect to all objectives. The resulting problem usually has a set of optimal solutions, known as Pareto-optimal solutions, non-inferior solutions, or effective solutions [49]. Since there exists more than one optimal solution and since without further information no one solution can be said to be better than any other Pareto-optimal solution, one of the goals of multi-objective optimization is to find as many Pareto-optimal solutions as possible. Within these multi-objective algorithms, there are two well-known types among others, such as (1) the non-dominated sorting genetic algorithm (NSGA-II) [50]. This algorithm sorts the population in different surfaces according to the Pareto dominance operator, but also using the so-called crowding distance, and (2) the multi-objective simulated annealing (MOSA) [51]. This algorithm is able to elicit a set of non-dominated solutions and it has been shown as a good meta-heuristic technique to evolve the model learning when multi-objective problems arise. In this study, the NSGA-II and the MOSA are used as the multi-optimization strategy.

6 A novel hybrid intelligent system for multi-objective machine parameter optimization in a dental milling process

The process of optimizing the manufacturing dental pieces in terms of time errors, based on the optimization of the system behavior, is carried out within the framework of this study by means of a hybrid intelligent system. The potential of this novel system is exemplified by the time error parameter and the temperature. The first parameter is chosen as an important factor in this process in terms of the economic benefit for a company. In the second case, a proper temperature in the manufacturing process would make it possible to obtain better quality products.

6.1 Identification of the relevant features

Firstly, the dental manufacturing process is parameterized and its dynamic performance in normal operation is obtained by the real process of manufacturing dental pieces. The gathered data is then pre-processed using projection models based on the analysis of parameters as the variance [34–36] or the kurtosis as CMLHL [31, 42]. This is done to identify internal data set structures to analyze whether the data set is sufficiently representative and to identify the most relevant features.

6.2 Modelling and optimization of a normal dental milling operation

Once the relevant variables and their transformations have been extracted from the production data, a model capable of fitting the normal manufacturing operation must be obtained. This is done to identify bias in the time error for manufacturing and the difference of temperature in the machine. The different model learning methods used in this study were implemented in Matlab© [52]. The model structures were analyzed to obtain the models that best suited the data set. Since the number of examples was small, a tenfold cross-validation schema was selected. The final model is obtained using all the data set.

Moreover, several different indexes were used to validate the models [20], such as the percentage representation of the estimated model, the graphical representation for the prediction ($\hat{y}_1(t|m)$) versus the measured output ($y_1(t)$), the loss function or error function (V) and the generalization error value.

The loss function or error function (V) is the numeric value of the MSE that is computed using the estimation data set by means of Eq. (6), while the generalization error value is the numeric value of the NSSE that is computed using the validation data set by means of Eq. (6). The percentage representation of the estimated model is calculated as the normalized mean error for the prediction (FIT1, FIT) using the validation data set and the complete data set, respectively, Eq. (7), where N is the number of samples of the data set used. Finally, the variance of the mean square errors (λ) is calculated [8].

$$J_1(m) = \frac{1}{N}\sum_{t=1}^{N} |y(t) - \hat{y}_1(t|m)|^2 \tag{6}$$

$$\text{FIT}\,(\%) = \left(1 - \frac{\sqrt{J_1(m)}}{\sqrt{\frac{1}{N}\sum_{t=1}^{N} |y(t)|^2}}\right) 100 \tag{7}$$

Once the model of the time error and the difference of temperature parameter in the machine for manufacturing dental pieces are selected, these models are used as two fitness functions in a multi-objective optimization with NSAGII and MOSA to obtain the best optimization of the time errors and changes of temperature. Both algorithms used in this study were implemented in Matlab© [53]. The complete novel hybrid intelligent system is shown in Fig. 2.

7 A real case scenario: a dental milling process optimization

Society demands esthetics, biocompatibility, and durability. This results in the need for fully adjusted dental treatments, with maximum strength and better appearance, but without limitation of materials or existing teeth situations (bridges, large structures, etc.,).

The development of technology in dentistry is advancing with the application of both industrial tools and computer science in this field (dental science).

The milling process in the preparation of dental prostheses is currently the most modern processing prosthesis in existence. This technique involves a process in which the frame molds for crowns and bridges are milled or polished from different material blocks.

The material (Cr–Co, Ti), the tools and the feed rates affect the conformation times. Since the processing involves polishing/milling the piece, the time of conformation determines its size. It is important to obtain the optimum diameter of the material block for minimizing tool wear and the loss of material.

Another important factor is the temperature of the milling tools, which can be expanded or fractured because of an inappropriate feed rate or because of the heating of the coolant. This could result in the inappropriate conformation of prosthetic restorations (crowns, bridges).

The industrial case scenario is based on the real data gathered by means of a Machining Milling Center of HERMLE type-C 20 U (iTNC 530), with swiveling rotary (280 mm), with a control system using high precision drills and bits, by optimizing the time error detection for manufacturing dental metal.

The real case study is described by an initial data set of 114 samples obtained by the dental scanner in the manufacturing of dental pieces with different tool types (plane, toric, spherical, and drill) characterized by 15 input variables (see Table 1). The input variables are the type of work, the thickness, the size of the tool, the radius of the tool, the tool, the number of pieces, the revolutions of the drill, the feed rate in each of the dimensions (X, Y and Z), the advance in the angle, the advance in the rotation, the initial tool diameter, the

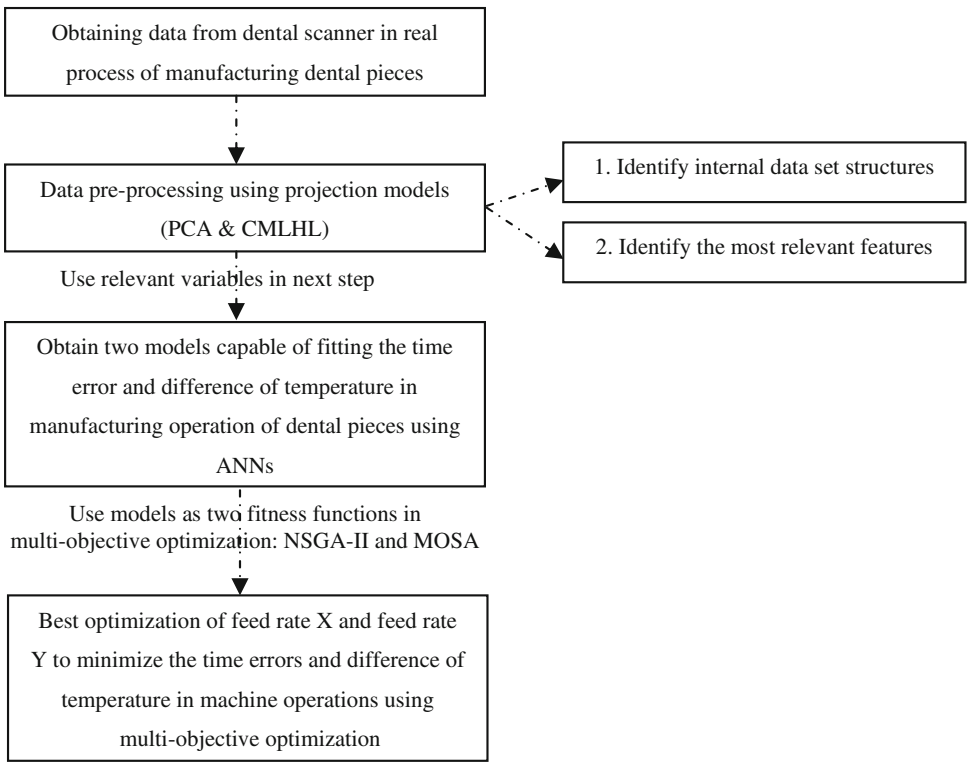

Fig. 2 A novel hybrid intelligent system to optimize a dental milling process

Table 1 Different features from the process, their units and ranges

Variable (units)	Range of values
Type of work (TW)	One locator attachment of cobalt-chromium (1), single-implant crown of cobalt-chromium (2), four-unit implant bridge of cobalt-chromium (3), single crown of cobalt-chromium (4), two-unit implant bridge of cobalt-chromium (5) and four crowns bridge of cobalt-chromium (6).
Thickness (mm) (T)	8 to 15
Size of tool (mm) (ST)	T2 to T23
Radius (mm) (R)	0.25 to 1.5
Tool (To)	Toric, spherical, plain, drill
Number of pieces (NP)	1 to 4
Revolutions per minute (RPM)	9,600 to 38,000
Feed rate *X* (mm per min) (FR *X*)	0 to 3,000
Feed rate *Y* (mm. per min) (FR *Y*)	0 to 3,000
Feed rate *Z* (mm per min) (FR *Z*)	75 to 2,000
Advance in angle (mm per min) (AA)	0 to 550
Advance in rotation (mm per min) (AR)	0 to 550
Initial diameter tool (mm) (ITD)	91.5035 to 110.4407
Initial temperature (°C) (IT)	24.8 to 30.4
Estimated work time (s) (EWT)	12 to 2,034
Time error for manufacturing (s) (TE)	−28 to −449
Difference of temperature in the machine (°C) (DT)	0.9 to 6.7
Difference of diameter of the tool (mm) (DD)	0.00080 to 0.11950

initial temperature and the estimated duration of the work.

There are two main parameters to estimate in this research: the time error for manufacturing and the difference of temperature in the machine. The time error for manufacturing is the difference between the estimated time by the machine itself and real work time (negative values indicate that real time exceeds estimated time). The difference of temperature in the machine is the difference between initial and final temperature in a dental milling process.

8 Results

This multidisciplinary research initially analyzed the data set to obtain the variables/characteristics that are most closely related to manufacturing time errors and difference of temperature in the machine.

In the first step, several unsupervised models were applied for the sake of comparison. In this case, neural versions of PCA and CMLHL were applied as powerful techniques for identifying internal data set structures. In order to analyze the two main parameters to be estimated (the time error for manufacturing and the difference of temperature in the machine) the initial data set was divided into two data sets: one with the time error and another with the difference of temperature.

The axes forming the projections (Figs. 3a, b, 4a, b) represent combinations of the variables contained in the original data sets. In the case of PCA, the model is looking for those directions with the biggest variance, while CMLHL is looking for the kurtosis (directions which are as little Gaussian as possible) [38, 42].

In relation to time error, (see Fig. 3), both methods, PCA (Fig. 3a) and CMLHL (Fig. 3b), are able to find a clear internal structure in the data set by identifying several clusters (see Tables 2, 3). Both methods also identified feed rate *X* and *Y* as relevant variables. It is clear that CMLHL provides a sparser representation than PCA, and that CMLHL projections provide more clear information identifying parameters, such as type of work and time error as other important variables.

An analysis of the results obtained with the CMLHL model (Fig. 3b) leads to the conclusion that this method has identified several different clusters ordered by feed rate *X* and *Y* and the type of work. Inside each cluster, there are further classifications by 'time error' and the data set can be said to have an interesting internal structure based on the clusters identified.

In relation to the difference of temperature, (see Fig. 4), both methods, PCA (Fig. 4a) and CMLHL (Fig. 4b), found a clear internal structure in the data set by identifying several clusters (see Tables 4, 5). It is clear that CMLHL provides a sparser representation than that obtained by PCA, and that CMLHL projections provide more clear information identifying parameters, such as the type of work, feed rate *X* and *Y*, initial temperature and difference of temperature as important variables.

An analysis of the results obtained with the CMLHL model (Fig. 4b) leads to the conclusion that this method has identified several different clusters ordered by the

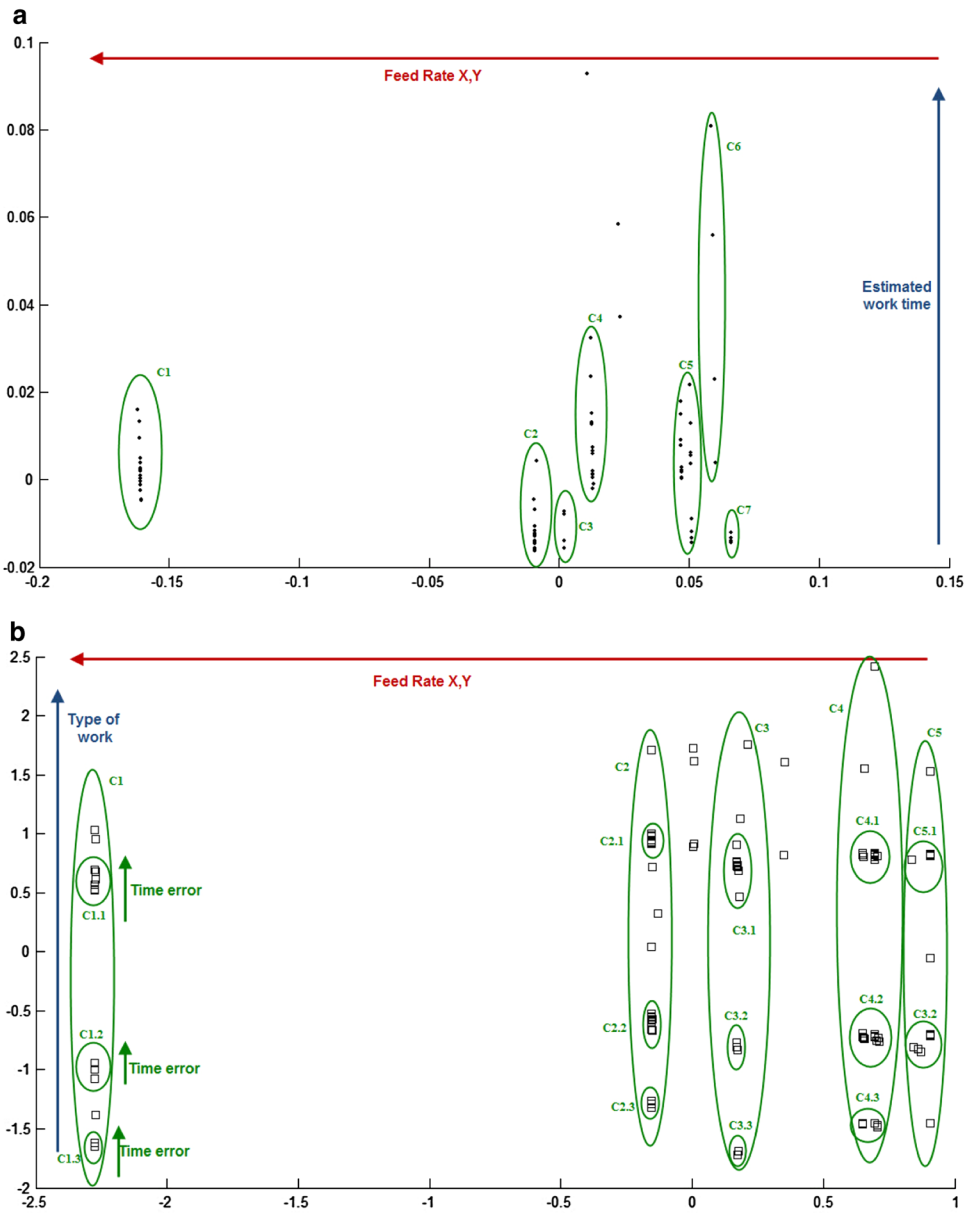

Fig. 3 PCA projection (**a**) and CMLHL projection (**b**) for data set with time error

difference of temperature and type of work. Inside each cluster, there are further classifications by 'feed rate *X*, *Y*' and 'initial temperature' and the data set can be said to have an interesting internal structure based on the clusters identified.

When the data set is considered sufficiently informative, as in this case, the next step is to model the relationship between inputs and production time errors, and between inputs and the difference of temperature in the process, which is accomplished by applying several artificial neural network modelling systems.

Two multilayer perceptron networks (MLP) (feedforward network) were used to monitor time error and the difference of temperature in the manufacturing of dental pieces. The data set is pre-processed from the input and output normalization step, and the reduction of the input vectors dimension (the data set gathered in the previous step). The MLP is trained from the most widely used training algorithms, such as the Levenberg–Marquardt algorithm [54], quasi-Newton methods [55], resilient backpropagation algorithm [56], and escalated conjugate gradient algorithm [57], using the criteria of normal stopping, early stopping, and Bayesian regularization techniques [58].

The features for the two best MLPs proposed and its indexes are stated below:

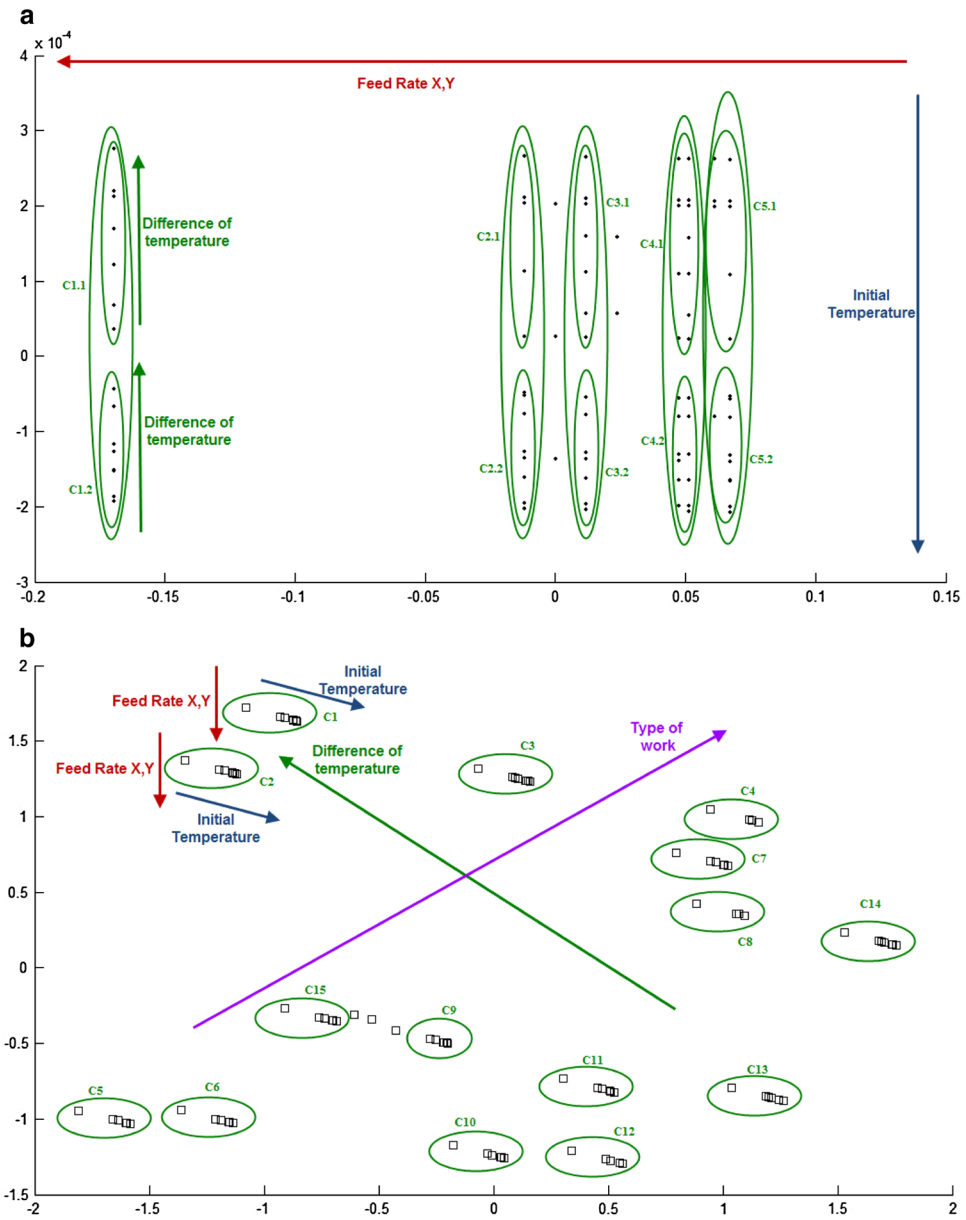

Fig. 4 PCA projection (**a**) and CMLHL projection (**b**) for data set with difference of temperature

Table 2 Samples description and clusters obtained using PCA method with time error

Cluster	Feed rate *X*, Feed rate *Y* (mm per min)	Estimated work time (s)
C1	3,000	From 660 to 378
C2	1,000	From 408 to 6
C3	850	From 168 to 12
C4	700	From 900 to 258
C5	250 and 200	From 690 to 12
C6	75	From 1,794 to 348
C7	0	From 48 to 6

The feedforward network—called f_1—to predict the time error has 30 hyperbolic tangent units (layer 1), 25 hidden hyperbolic tangent units (layer 2), 25 hidden hyperbolic tangent units (layer 3), 4 hidden hyperbolic tangent units (layer 4), and 1 linear output unit. The parameters in the network were estimated using the Levenberg–Marquardt algorithm with normal stopping criterion. Normalizing the minimum and maximum values of data set to $[-1\ 1]$.

The feedforward network—called f_2—to predict the difference of temperature has 30 hyperbolic tangent units (layer 1), 20 hidden hyperbolic tangent units (layer 2), 5

Table 3 Samples description and clusters obtained using CMLHL method with time error

Cluster	Type of work	Time error (s)	Feed rate *X*, *Y* (mm per min)
C1			
C1.1	4	From −238 to −202	3,000
C1.2	2	From −317 to −227	
C1.3	1	From −218 to −211	
C2			
C2.1	4	From −98 to −42	1,000
C2.2	2	From −44 to −71	
C2.3	1	From −51 to 306	
C3			
C3.1	4	From −128 to −43	700
C3.2	2	From −86 to −75	
C3.3	1	From −110 to −104	
C4			
C4.1	4	From −46 to −33	250 and 200
C4.2	2	From −46 to −35	
C4.3	1	From −39 to −35	
C5			
C5.1	4	From −36 to −28	75 and 0
C5.2	2	From −45 to −30	

Table 4 Samples description and clusters obtained using PCA method with difference of temperature

Cluster	Difference of temperature (°C)	Initial temperature (°C)	Feed rate *X*, *Y* (mm per min)
C1			
C1.1	From 6.7 to 0.7	From 24.1 to 25.7	3,000
C1.2	From 3.3 to 0.9	From 28.1 to 31	
C2			
C2.1	From 6.7 to 0.7	From 24.1 to 25.3	1,000
C2.2	From 3.8 to 0.9	From 28.4 to 31	
C3			
C3.1	From 6.7 to 0.7	From 24.1 to 25.7	700
C3.2	From 3.3 to 0.9	From 28.4 to 31	
C4			
C4.1	From 6.7 to 0.7	From 24.1 to 25.7	250 and 200
C4.2	From 3.3 to 0.9	From 28.4 to 31	
C5			
C5.1	From 6.7 to 0.7	From 24.1 to 25.3	75 and 0
C5.2	From 3.8 to 0.9	From 28.4 to 31	

hidden hyperbolic tangent units (layer 3), and 1 linear output unit. The parameters in the network were estimated using the Levenberg–Marquardt algorithm with Bayesian regularized criterion. Normalizing the data set to media null and variance 1.

These models (f_1 and f_2) do not only present the lowest *V* (0.001 and 5.25E−5) and NSSE (0.013 and 0.12E−3), but also a higher system representation index value FIT1 (82.45 and 99.87 %) and a small λ(0.1E−4 and 1.32E−9). From these indicators, it may be concluded that the ANNs selected are able to simulate and predict the behavior of time errors and the difference of temperature for manufacturing dental pieces (as a consequence of the production process).

Table 5 Samples description and clusters obtained using CMLHL method with difference of temperature

Cluster	Difference of temperature (°C)	Type of work	Initial temperature (°C)
C1	6.7	2	24.1
C2	6.7	2	25.3
C3	5.6	4	24.8
C4	4.7	6	25.2
C5	3.3	1	31
C6	2.4	1	30.4
C7	3	4	25
C8	2.3	4	25.7
C9	2.7	2	28.4
C10	2	4	31
C11	1.7	4	29.3
C12	0.9	4	30.4
C13	0.9	5	29
C14	0.7	4	25.3
C15	3.3	2	28.7

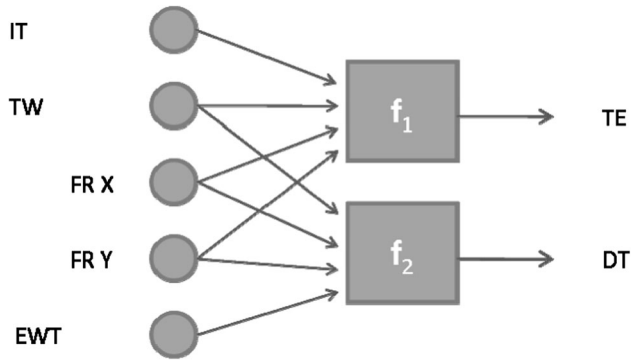

Fig. 5 Multi-objective optimization NSGA-II and MOSA for the variables TE and DT. IT, TW, and EWT are values fixed. The values FR *X* and FR *Y* are obtained

The models of time error (f_1) and difference of temperature (f_2) obtained may be used as two fitness functions in the next step to determine the best operating conditions for the dental milling processes, i.e., to choose the values of feed rate *X* and feed rate *Y* with the least possible time error and the least change of temperature in the process.

Figure 5 shows the representation of this optimization process. Where IT, TW, and EWT are values fixed and FR *X* and FR *Y* are values obtained when TE and DT are close to zero.

For the problem, 11 experiments have been designed and 10 runs of each experiment have been carried out for statistics purposes. The experiments use a population size of 100 individuals, 200 iterations for the NSGA-II [and a bigger number of iterations for the MOSA (200, 500, and 1,000 in some experiments)]. The crossover probabilities are 0.8 and mutation probabilities are 0.2. MOSA uses $\Delta = 0.1$, $T_0 = 1$, and $T_1 = 0.01$. The results are shown in Table 6 and in the boxplot of Fig. 6. In Table 6, the 11 experiments are compared for the best individual error found and for the individual closest to the origin. Although some differences have been found, both the MOSA and the NSGA-II are valid to learn the models. Nevertheless, the NSGA-II presents a worst behavior in the MSE of time error in some experiments.

Besides, in Fig. 7 is depicted one of the multi-optimization experiments accomplished and shown in the Table 6, concretely the experiment number five. The *X*-axis shows the feed rate *X* (mm per min) and the *Y*-axis represents feed rate *Y* (mm per min), for from 0 to 3,000. The features fixed are 29 °C for initial temperature and 900 s for estimated work time. In Fig. 7a, the *Z*-axis represents the output variable range (time error) from −3,000 to 1,000 s. This value is also shown on the vertical bar. In Fig. 7c, the *Z*-axis represents the output variable range (difference of temperature) from −8 to 4 °C. The difference in temperature is also shown on the vertical bar. Figure 7b, d presents the final value got for the feed rate *X* and *Y* with a value close to zero in the two outputs optimized (the black point in the interior of circle).

9 Conclusions and future work

The novel hybrid intelligent system with a multi-objective optimization process described in this research can be successfully used to optimize machine parameters for industrial processes, based on the obtained results. The optimization process may increase a company's efficiency and substantially reduces the cost of preparing and setting machine processes. We have used this method for multi-objective optimization and adjustments during the manufacturing process of dental pieces, such as implants according to medical specifications for precise moldings.

The method proposed is based on the selection of the most important features in an initial step. ANNs are then trained for modelling the features and these can, thus, be used as two fitness functions in the multi-objective optimization. Finally, a NGSA-II and MOSA try to achieve the best conditions for manufacturing from the model.

Table 6 Experimentation results for manufacturing under different conditions in the dental milling process

Algorithm used		Execution	Values fixed			Values obtained for the closest to the origin				MSE	
Experiments		Time (m)	TW	IT	EWT	FR *X*	FR *Y*	DT	TE	DT	TE
1	**NII**	**41**	1	31	12	**1,111.36**	**1,663.99**	**4.43E−09**	**2.31E−11**	2E−05	6.74E−11
	M(200)	229	1	31	12	419.31	718.48	2.217	−0.12	4.389	4.317
2	**NII**	**43**	2	28.7	12	**784.58**	**1,517.3**	**−0.883**	**−0.20**	13.822	1.778
	M(200)	141	2	28.7	12	803.13	1,633.81	−1.126	1.16	13.265	5.181
	M(500)	456	2	28.7	12	740.88	1,431.94	−0.903	−0.86	4.33	1.434
	M(1000)	4,380	2	28.7	12	806.80	1,695.88	−1.33	−0.259	2.489	0.908
3	**NII**	**41**	3	25.7	366	**839.08**	**939.69**	**0.182**	**6.94E−06**	0.077	1.62E−03
	M(200)	119	3	25.7	366	874.71	788.15	0.366	0.184	0.107	9.539
4	**NII**	**46**	4	28.4	378	**449.29**	**1,305.34**	**−3.2E−05**	**7.03E−08**	0.131	54,859.73
	M(200)	66	4	28.4	378	453.11	646.09	0.0059	0.123	1.089	1.638
5	**NII**	**45**	5	29	900	**953.86**	**1,132.3**	**−4.4E−15**	**3.27E−13**	0.00015	1.05E−06
	M(200)	65	5	29	900	434.11	646.09	0.038	0.448	0.154	34.68
6	**NII**	**45**	6	25.2	1,380	**498.13**	**1,711.1**	**1.784**	**0.0002**	8.703	23,273.33
	M(200)	88	6	25.2	1,380	971.64	2,045.09	1.353	0.0065	4.734	12.229
7	**NII**	**45**	1	30.4	282	**192.96**	**475.59**	**1.265**	**0.021**	3.504	0.648
	M(200)	80	1	30.4	282	646.45	870.97	1.355	−0.103	2.133	0.114
8	**NII**	**44**	6	25.2	660	**117.39**	**1,709.47**	**0.0019**	**−0.00017**	11.263	11,141.42
	M(200)	54	6	25.2	660	142.19	1,671.5	0.412	−2.534	6.430	66.352
9	**NII**	**44**	2	28.7	66	**904.5**	**1436**	**4.88E−15**	**−1.14E−13**	6.3E−07	7.62E−12
	M(200)	49	2	28.7	66	763.53	1,245.88	−0.156	0.287	3.541	11.938
	M(500)	253	2	28.7	66	829.46	1,284.11	0.088	−0.181	0.254	6.290
10	**NII**	**45**	3	28.4	378	**66.78**	**1,266.11**	**0.173**	**0.029**	1.09	0.019
	M(200)	81	3	28.4	378	60	1,266.19	0.156	−1.602	4.34	6.103
	M(500)	240	3	28.4	378	749.68	1,011.99	2.627	0.136	7.37	2.47
11	**NII**	**45**	6	25.2	2,034	**1,631.99**	**1,090.45**	**2.686**	**0.011**	7.506	0.041
	M(200)	117	6	25.2	2,034	572.99	1,264.7	3.199	0.413	11,519	9.164

MSE value of the mean central point of the MSE function for the individuals of lowest MSE value individual in the populations (MSE) and the closest to the origin individual in the populations, considering the 10 runs of each experiment

M MOSA, *NII* NSGA-II

Bold type depicts the execution time and the best values obtained for the closest to the origin in DT and TE for each experiment

The data set collected in this real dental milling process presents an important manufacturing time error rate of about 26.8 %. This is due to the difference between the estimated time of the machine itself and the real production time. The obtained model is capable of modelling more than 82 % of the actual measurements in relation to the time error (modelling more than 96.1 % of real time work). This helps to reduce the error and the variability rate of manufacturing processes down to 4 %, compared to the initial 26.8 %, which is an acceptable error rate in planning work for dental milling. In addition, the difference of temperature between the beginning and the end of the dental manufacturing process has an increase of about 10.2 %. The obtained model is capable of modelling more than 99 % of the actual measurements in relation to the difference of temperature (modelling more than 99 % of real final temperature work).

The multi-objective optimization is able to find the best values for the feed rate *X* and *Y* from some fixed parameters, such as normal conditions of manufacturing and the multi-objective minimization of time errors, and the difference of temperature. Although, both the MOSA and the NSGA-II are valid to learn the models, the best results—considering the 10 runs—are obtained in less time with NSGA-II; i.e., the solution can be obtained with less computational cost. Therefore, the milling process will be able to minimize the time errors and the difference of temperature to a value as close to zero as possible.

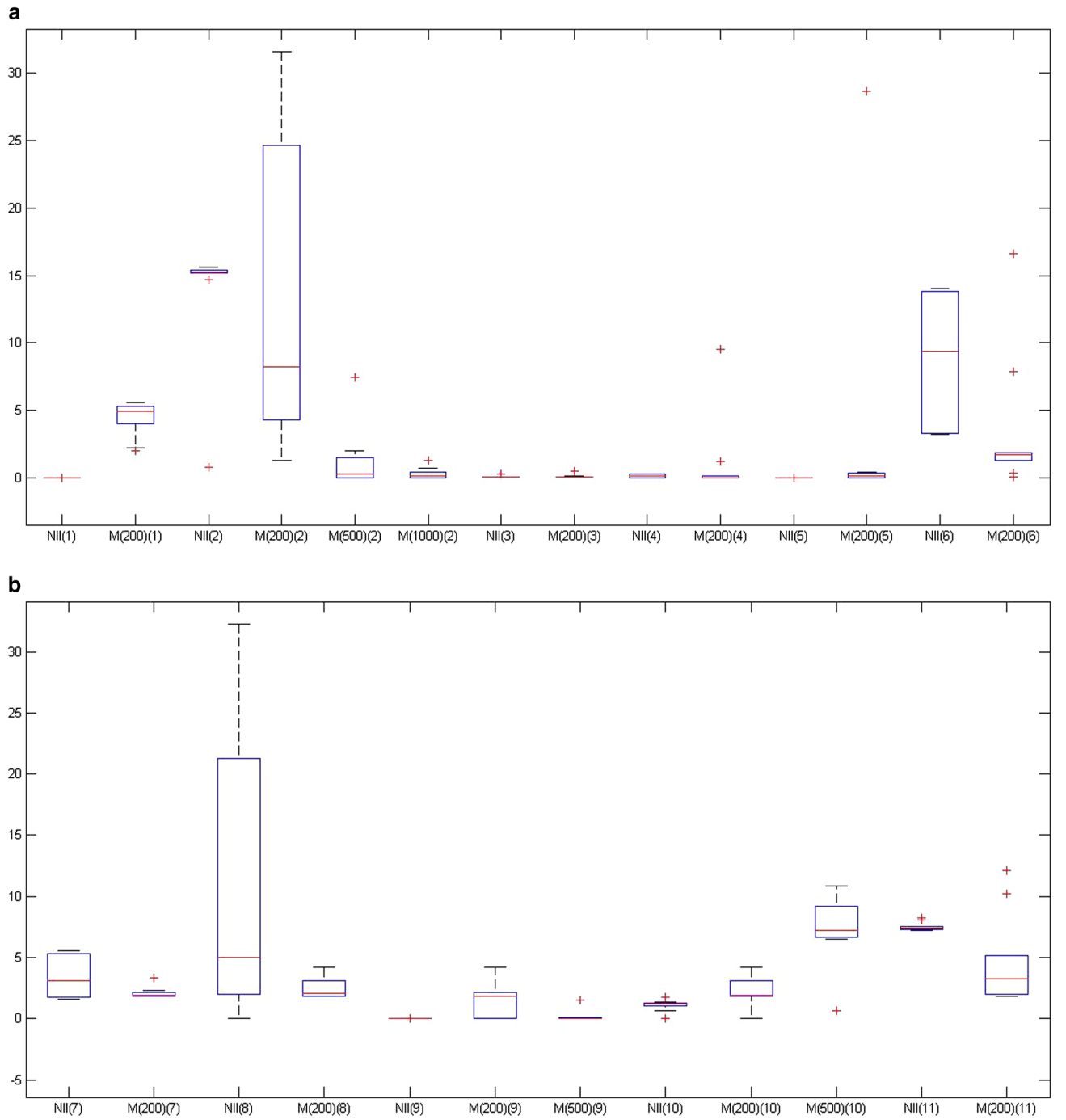

Fig. 6 Boxplot of the central points of the MSE for the best individuals considering only the MSE function in DT. Each box is identified using M for MOSA or N for NSGA-II and a number for the experiment

Future lines of research will investigate the selection of the most suitable features using a wrapper feature selection method, in which Genetic Algorithms and ANNs are hybridized. Finally, an algorithm will be developed to automatically identify the best operating conditions: minor time errors for the manufacturing of dental pieces and minor differences of temperature. Moreover, the resulting model would be applied to different metals used in prosthetic dentistry and in other industrial processes, such as the automotive sector.

Acknowledgments This research is partially supported through projects of the Spanish Ministry of Economy and Competitiveness [ref: TIN2010-21272-C02-01 (funded by the European Regional Development Fund), TIN2008-06681-C06-04 and SA405A12-2 from Junta de

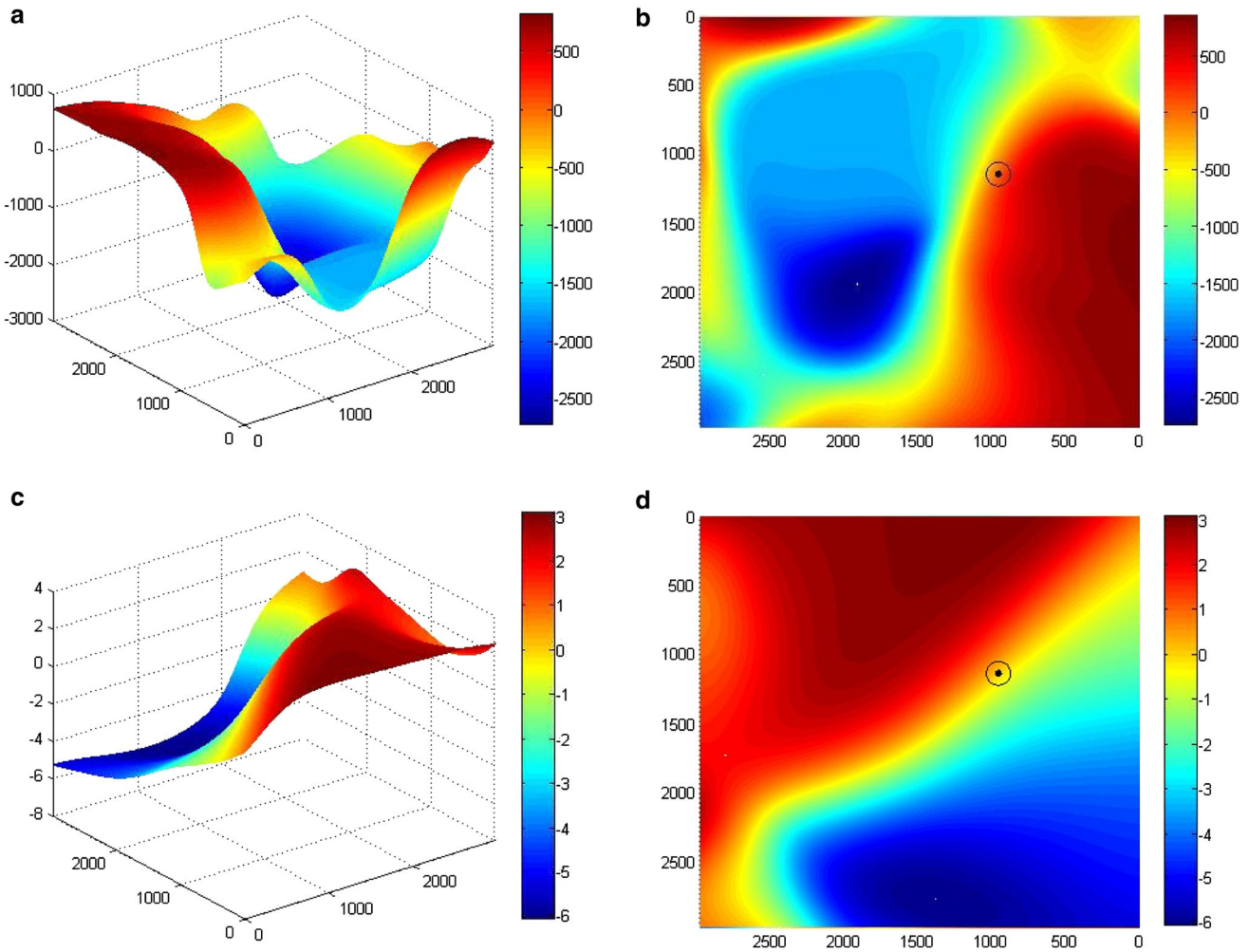

Fig. 7 Output response of the time error and the difference of temperature for different input variable ranges in the manufacturing of two unit implant bridges of cobalt-chromium. **a** 3D graph, the *X*-axis represents feed rate *X*, the *Y*-axis is the feed rate *Y* and the *Z*-axis the output (time error). **b** 2D graph, the *X*-axis represents feed rate *X* and the *Y*-axis is the feed rate *Y*. The *black point* is the chosen output (time error). **c** 3D graph, the *X*-axis represents feed rate *X*, the *Y*-axis is the feed rate *Y* and the *Z*-axis the output (difference of temperature). **d** 2D graph, the *X*-axis represents feed rate *X* and the *Y*-axis is the feed rate *Y*. The *black point* is the chosen output (difference of temperature)

Castilla y León]. The authors would also like to thank to ESTUDIO PREVIO (Madrid-Spain) for its collaboration in this research.

References

1. Corchado E, Sedano J, Curiel L, Villar JR (2012) Optimizing the operating conditions in a high precision industrial process using soft computing techniques. Expert Systems 29(3):276–299. http://dx.doi.org/10.1111/j.1468-0394.2011.00588.x
2. Frank M, Hamprecht F (2011) Image-based supervision of a periodically working machine. Pattern Anal Appl 1–10. http://dx.doi.org/10.1007/s10044-011-0245-7
3. Huang L, Suh IH, Abraham A (2011) Dynamic multi-objective optimization based on membrane computing for control of time-varying unstable plants. Inf Sci 181(11):2370–2391
4. Das MK, Kishor N (2009) Adaptive fuzzy model identification to predict the heat transfer coefficient in pool boiling of distilled water. Expert Syst with Appl 36(2, Part 1):1142–1154
5. Esen H, Inalli M (2009) Modelling of a vertical ground heat pump system by using artificial neural networks. Expert Syst Appl 36(7):10229–10238
6. Ljung L (1999) System identification, theory for the user, 2nd edn. Prentice-Hall, Upper Saddle River
7. Sedano J, Corchado E, Curiel L, Villar J, Bravo PM (2009) The application of a two-step AI model to an automated pneumatic drilling process. Int J Comput Math 86(10):1769–1777
8. Sedano J, Curiel L, Corchado E, de la Cal E, Villar JR (2010) A soft computing based method for detecting lifetime building thermal insulation failures. Integr Comput-Aided Eng 17(2): 103–115
9. Vera V, Corchado E, Redondo R, Sedano J, García ÁE (2013) Applying soft computing techniques to optimise a dental milling process. Neurocomputing 109:94–104. http://dx.doi.org/10.1016/j.neucom.2012.04.033
10. Kalyani S, Swarup K (2012) Design of pattern recognition system for static security assessment and classification. Pattern Anal Appl 15 (3):299–311. http://dx.doi.org/10.1007/s10044-011-0218-x

11. Miyazaki T, Hotta Y, Kunii J (2009) A review of dental CAD/CAM: current status and future perspectives from 20 years of experience. Dent Mater J 28(1):44–56
12. Fuster-Torres MA, Albalat-Estela S, Alcañiz-Raya M, Peñarrocha-Diago M (2009) CAD/CAM dental systems in implant dentistry: Update. Med Oral Patol Oral Cir Bucal 14(3):E141–E145
13. Beuer F, Schweiger J, Edelhoff D (2008) Digital dentistry: an overview of recent developments for CAD/CAM generated restorations. Br Dent J 204(9):497–502
14. Weaver J, Johnson G, Bales D (1991) Marginal adaptation of castable ceramic crowns. J Prosthet Dent 66:747–753
15. (2005) Glossary of Prosthodontic Terms. J Prosthet Dent 94: 92
16. Wolfart S, Martin S, Kern M (2003) Clinical evaluation of marginal fit of a new experimental all—ceramic system before and after cementation. Int J Prosthodont 6:587–592
17. Francine E, Omar M (2004) Marginal adaptation and microleakage of Procera All Ceram crowns with four cements. Int J Prosthodont 17:529–535
18. McLean J, von Fraunhofer JA (1971) The estimation of cement film by an in vivo technique. Br Dent J 131:107–111
19. Karlsson S (1993) The fit of Procera titanium crowns. An in vitro and clinical study. Acta Odontol Scand 51:129–134
20. Vera V, Sedano J, Corchado E, Redondo R, Hernando B, Camara M, Laham A, Garcia AE (2011) A hybrid system for dental milling parameters optimisation. In: 6th International conference on hybrid artificial intelligence systems. Wroclaw, Poland HAIS 2011, Part II, LNAI 6679, pp 437–446
21. Corchado E, Graña M, Wozniak M (2012) Editorial: new trends and applications on hybrid artificial intelligence systems. Neurocomputing 75(1):61–63
22. Chang Hsu-Hwa, Chen Yan-Kwang (2011) Neuro-genetic approach to optimize parameter design of dynamic multiresponse experiments. Appl Soft Comput 11(1):436–442
23. Corchado E, Abraham A, Ponce Leon Ferreira de Carvalho AC (2010) Hybrid intelligent algorithms and applications. Inf Sci 180(14):2633–2634
24. Abraham A, Corchado E, Corchado JM (2009) Hybrid learning machines. Neurocomputing 72(13–15):2729–2730
25. Borrajo ML, Baruque B, Corchado E, Bajo J, Corchado JM (2011) Hybrid neural intelligent system to predict business failure in small-to-medium-size enterprises. Int J Neural Syst 21(4):277–296
26. Fujita S (2009) Retrieval parameter optimization using genetic algorithms. Inf Process Manage 45:664–682
27. Oliveira ALI, Braga PL, Lima RMF, Cornélio ML (2010) Ga-based method for feature selection and parameters optimization for machine learning regression applied to software effort estimation. Inf Softw Technol 52:1155–1166
28. Dorigo M, Stützle T (2004) Ant Colony Optimization. Bradford Co, Scituate
29. Liu Y, Zhou C, Guo D, Wang K, Pang W, Zhai Y (2010) A decision support system using soft computing for modern international container transportation services. Appl Soft Comput 10(4):1087–1095
30. Twycross J, Aickelin U (2010) Information fusion in the immune system. Inf Fusion 11(1):35–44
31. Corchado E, Herrero A (2011) Neural visualization of network traffic data for intrusion detection. Appl Soft Comput 11(2): 2042–2056
32. Fougères A (2011) Modelling and simulation of complex systems: an approach based on multi-level agents. IJCSI Int J Comput Sci Issues 8(6):8–17
33. Castro JL, Navarro M, Sánchez JM, Zurita JM (2009) Loss and gain functions for CBR retrieval. Inf Sci 179(11):1738–1750
34. Pearson K (1901) On lines and planes of closest fit to systems of points in space. Phil Mag 2(6):559–572
35. Hotelling H (1933) Analysis of a complex of statistical variables into Principal Components. J Educ Psychol 24:417–444
36. Oja E, Ogawa H, Wangviwattana J (1992) Principal components analysis by homogeneous neural networks, part 1, the weighted subspace criterion. IEICE Trans Inf Syst E75D:366–375
37. Diaconis P, Freedman D (1984) Asymptotics of graphical projections. Ann Stat 12(3):793–815
38. Corchado E, MacDonald D, Fyfe C (2004) Maximum and minimum likelihood hebbian learning for exploratory projection pursuit. Data Min Knowl Disc 8(3):203–225
39. Friedman JH (1987) Exploratory projection pursuit. J Am Stat Assoc 82(397):249–266
40. Pedrycz W, Lee D, Pizzi N (2010) Representation and classification of high-dimensional biomedical spectral data. Pattern Anal Appl 13(4):423–436
41. Gunala S, Edizkanb R (2008) Subspace based feature selection for pattern recognition. Inf Sci 178(19):3716–3726
42. Corchado E, Fyfe C (2003) Connectionist techniques for the identification and suppression of interfering underlying factors. Int J Pattern Recognit Artif Intell 17(8):1447–1466
43. Fyfe C, Corchado E (2002) Maximum likelihood hebbian rules. In: Verleysen M (ed) Proceedings of the 10th Eurorean Symposium on Artificial Neural Networks, Bruges, Belgium, April 24-26 (ESANN 2002), pp 143–148
44. Corchado E, Han Y, Fyfe C (2003) Structuring global responses of local filters using lateral connections. J Exp Theor Artif Intell 15(4):473–487
45. Seung H, Socci N, Lee D (1998) The rectified Gaussian distribution. Adv Neural Inf Process Syst 10:350–356
46. Nørgaard M, Ravn O, Poulsen NK, Hanse LK (2000) Neural networks for modelling and control of dynamic systems. Springer-Verlag, London
47. Schoukens J, Rolain Y, Pintelan R (2004) Improved approximate identification of nonlinear systems. In: 21st IEEE instrumentation and measurement technology conference, Como, Italy, pp 2183–2186
48. Hanne T (2000) Global multi-objective optimization using evolutionary algorithms. J Heuristics 6(3):347–360
49. Srinivas N, Deb K (1995) Multi-objective function optimization using nondominated sorting genetic algorithms. Evol Comput J 2(3):221–248
50. Deb K, Pratap A, Agarwal S, Meyarivan T (2000) A fast elitist multi-objective genetic algorithm: NSGA-II. IEEE Trans Evol Comput 6:182–197
51. Luciano Sánchez L, Villar JR (2008) Obtaining transparent models of chaotic systems with multi-objective simulated annealing algorithms. Inf Sci 178:952–970
52. Demuth H, Beale M, Hagan M (2010) Neural Network Toolbox User's Guide. The Mathworks Inc., Natick
53. The Math Works. Global Optimization Toolbox. The MathWorks Inc., URL: http://www.mathworks.com/products/global-optimization/index.html
54. Fletcher R (1987) Practical methods of optimization, 2nd edn. Wiley & Sons, Chichester
55. Dennis JE, Schnabel RB (1983) Numerical methods for unconstrained optimization and nonlinear equations. Prentice-Hall, Englewood Cliffs
56. Riedmiller M, Braun H (1993) A directive adaptive method for faster backpropagation learning: The RPROP algorithm. In: Proceedings for IEEE International Conference on Neural Networks
57. Moller MF (1993) A scaled conjugate gradient algorithm for fast supervised learning. Neural Netw 6:525–533
58. Mackay DJC (1992) Bayesian interpolation. Neural Comput 4(3):415–447